



ELSEVIER

Contents lists available at ScienceDirect

## Free Radical Biology and Medicine

journal homepage: [www.elsevier.com/locate/freeradbiomed](http://www.elsevier.com/locate/freeradbiomed)

## Original Contribution

## Visualizing and quantifying oxidized protein thiols in tissue sections: A comparison of dystrophic mdx and normal skeletal mouse muscles

Tomohito Iwasaki<sup>a</sup>, Jessica Terrill<sup>a,b</sup>, Tea Shavlakadze<sup>a</sup>, Miranda D. Grounds<sup>a</sup>, Peter G. Arthur<sup>b,\*</sup><sup>a</sup> School of Anatomy, Physiology and Human Biology, University of Western Australia, Perth, WA 6009, Australia<sup>b</sup> School of Chemistry and Biochemistry, University of Western Australia, Perth, WA 6009, Australia

## ARTICLE INFO

## Article history:

Received 29 April 2013

Received in revised form

9 August 2013

Accepted 25 September 2013

Available online 3 October 2013

## Keywords:

Reactive oxygen species

Oxidative stress

Histochemistry

Protein thiol

Sulfhydryl

Murine

Skeletal muscle

Muscular dystrophy

Free radicals

## ABSTRACT

Reactive oxygen species (ROS) are not only a cause of oxidative stress in a range of disease conditions but are also important regulators of physiological pathways *in vivo*. One mechanism whereby ROS can regulate cell function is by modification of proteins through the reversible oxidation of their thiol groups. An experimental challenge has been the relative lack of techniques to probe the biological significance of protein thiol oxidation in complex multicellular tissues and organs. We have developed a sensitive and quantitative fluorescence labeling technique to detect and localize protein thiol oxidation in histological tissue sections. In our technique, reduced and oxidized protein thiols are visualized and quantified on two consecutive tissue sections and the extent of protein thiol oxidation is expressed as a percentage of total protein thiols (reduced plus oxidized). We tested the application of this new technique using muscles of dystrophic (mdx) and wild-type C57Bl/10Scsn (C57) mice. In mdx myofibers, protein thiols were consistently more oxidized ( $19 \pm 3\%$ ) compared with healthy myofibers ( $10 \pm 1\%$ ) in C57 mice. A striking observation was the localization of intensive protein thiol oxidation ( $70 \pm 9\%$ ) within myofibers associated with necrotic damage. Oxidative stress is an area of active investigation in many fields of research, and this technique provides a useful tool for locating and further understanding protein thiol oxidation in normal, damaged, and diseased tissues.

© 2013 Elsevier Inc. All rights reserved.

Oxidative stress, caused by the generation of reactive oxygen species (ROS)<sup>1</sup>, is evident in a range of physiological and pathological conditions. Some ROS, such as hydroxyl radicals, can affect cellular function by irreversibly damaging macromolecules such as proteins, lipids, and nucleic acids [1,2]. A number of analytical techniques have been developed to directly measure oxidation products such as the carbonylation of proteins or products of degradation pathways such as F<sub>2</sub>-isoprostanes [3–5]. These analytical techniques are used to monitor the physiological and pathological effects of oxidative stress in animal models and human tissues.

An alternate pathway by which some ROS (e.g., hydrogen peroxide) can affect cellular function is through the biologically reversible oxidation of protein thiol groups, to form, for example, intramolecular disulfide bonds. On the basis of studies performed

with purified proteins and experimental models utilizing cultured cells, it is evident that the function of many proteins can be affected by reversible thiol oxidation, including proteins involved in signal transduction, ion transport, contraction, metabolism, protein synthesis, protein catabolism, and regulation of gene expression [6–8]. The significance of changes to cell function caused by protein thiol modifications is well established in cell culture systems [9,10]. However, there is still a paucity of information on the extent and location of reversible protein thiol oxidation in animal models and humans mainly because of the technical difficulties in measuring highly labile protein thiol groups in tissue samples [11].

Recently, we developed a highly sensitive dual-labeling method to measure the global level of reversible protein thiol oxidation level in tissues from animal models [2,6,12]. Using this technique, we established that protein thiol oxidation was elevated in dystrophic muscle from *mdx/mdx* (mdx) mice [2,13,14]. Furthermore, the lack of correlation between the level of protein thiol oxidation and other more traditional markers of oxidative stress, such as malondialdehyde or protein carbonylation, indicates that the impact of oxidative stress is manifested differentially between irreversible oxidative damage pathways and biologically reversible protein thiol oxidation [2]. This indicates that direct measurement

**Abbreviations:** A.U., arbitrary units; C57, C57Bl/10Scsn; FLm, BODIPY FL-N-(2-aminoethyl)maleimide; NEM, N-ethylmaleimide; PBS, phosphate-buffered saline; PFA, paraformaldehyde; PVA, polyvinyl acetate; ROS, reactive oxygen species; SDS, sodium dodecyl sulfate; TCA, trichloroacetic acid; TCEP, tris(2-carboxyethyl)phosphine; H&E, hematoxylin and eosin

\* Corresponding author.

E-mail address: [peter.arthur@uwa.edu.au](mailto:peter.arthur@uwa.edu.au) (P.G. Arthur).

of protein thiols would be preferable when there is an interest in the effects of oxidative stress on protein thiols.

The dual-labeling method utilizes tissue homogenates to provide information on the extent of reversible protein thiol oxidation in the target tissue [2,13]. Many organs have a complex composition of cell types, so techniques utilizing tissue homogenates do not provide information on potential regional variations in the level of protein thiol oxidation. A histological technique to evaluate one form of thiol oxidation has been developed, and it involves detecting linkages between proteins and glutathione (glutathionylation) in cultured cells [15]. However, this technique does not detect other forms of reversible thiol oxidation (e.g., intramolecular disulfide formation), nor has it been tested in animal tissues *in vivo*. These issues are addressed in the present study, which describes the development of a novel histological technique to visualize and measure the extent of protein thiol oxidation in tissue. To validate the technique for tissue sections, we have utilized muscle tissue from mice primarily because we have expertise in working with *in vivo* mouse models of muscle disorders, particularly dystrophic mdx mice, and have shown that protein thiol oxidation is elevated in dystrophic muscles [16]. We show that this new thiol histological technique provides information about the location of protein thiol oxidation that cannot be obtained by using a tissue homogenate method.

## Materials and methods

### Animals

All experiments were carried out on adult male dystrophic mdx and nondystrophic control C57Bl/10Scsn (C57) mice ages 12–15 weeks, purchased from the Animal Resources Centre, Western Australia. All mice were housed at the University of Western Australia under specific-pathogen-free conditions on a 12-h light/dark cycle, with free access to food and drinking water. All animal experiments were conducted in accordance with the guidelines of the National Health and Medical Research Council of Australia Code of Practice for the Care and Use of Animals for Scientific Purposes (2004) and the Animal Welfare Act of Western Australia (2002) and were approved by the Animal Ethics Committee at the University of Western Australia.

### Tissue collection

Mice were killed at 12 or 15 weeks of age by cervical dislocation while under terminal anesthesia (2% isoflurane; Bomac, Australia). Quadriceps femoris and triceps branchii muscles were collected while the mice were under terminal anesthesia, mounted onto tragacanth gum (Sigma), and frozen in isopentane (Sigma) quenched in liquid nitrogen for cryosectioning.

### Histological labeling for comparison of the thiol reduction/oxidation state of proteins

An overview of the labeling protocol is described in Fig. 1. All incubations were performed in the dark to prevent degradation of the fluorescent signal. Three consecutive transverse serial sections (9 μm) were cut on a cryostat (Leica Microsystems CM3050) at –20 °C and collected onto precooled slides (–20 °C for 20 min) to minimize artifactual oxidation. Section 1 was immediately (estimated to be less than 10 s from the time of cutting) treated with 0.225 mM BODIPY FL-N-(2-aminoethyl)maleimide (FLm; Invitrogen, USA) in 0.5 M Tris-HCl (pH 7.0) and incubated for 30 min at room temperature. Sections 2 and 3 were immediately treated with 200 mM N-ethylmaleimide (NEM) in 0.5 M Tris-HCl (pH 7.0) and incubated

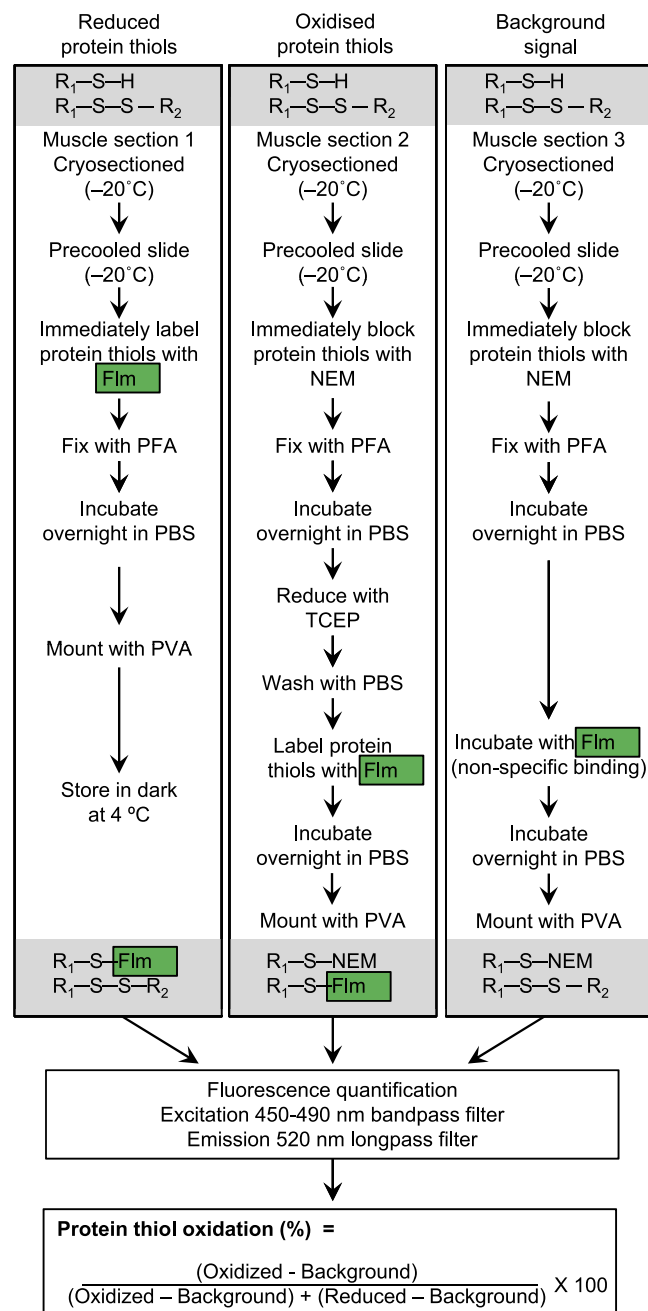


**Fig. 1.** Overview of protein thiol labeling protocol. To minimize artifactual oxidation, cryosections were processed immediately after cutting. Cryosections were reacted either with FLm to visualize reduced protein thiols or with NEM to visualize oxidized protein thiols or to account for nonspecific binding by FLm (background signal). Oxidized thiols (including disulfides) in the NEM-reacted tissue section were reduced with TCEP and then labeled with FLm to visualize oxidized protein thiols. Details are described under Materials and methods.

for 30 min at room temperature. All sections were then washed three times in phosphate-buffered saline (PBS) at pH 7.0 to remove excess FLm or NEM. Sections were fixed with 4% paraformaldehyde (PFA) in 0.1 M phosphate buffer, pH 7.4, for 30 min at room temperature. PFA was removed by washing two times for 5 min with PBS and then incubating in PBS overnight at room temperature. Section 1 was then mounted with polyvinyl acetate (PVA) and stored at 4 °C until analysis 1 day later. Section 2 was reduced with 200 mM tris(2-carboxyethyl)phosphine (TCEP) in 0.5 M Tris-HCl (pH 7.0) for 1 h at room temperature and then rapidly (< 1 min) washed two times with precooled PBS at 4 °C. Section 2 was then immediately labeled

with 0.2 mM FLm in 0.5 M Tris–HCl (pH 7.0) for 30 min at room temperature. Section 3 was incubated with FLm concurrent with section 2 and incubated in PBS overnight at room temperature. Sections 2 and 3 were then mounted with PVA and all sections (1–3) were fluorescently imaged. Other serial sections were routinely stained with hematoxylin and eosin (H&E) for morphological analyses.

#### Microscope imaging and image analysis

Fluorescence images were acquired using a Nikon Eclipse Ti microscope equipped with a CoolSNAP-HQ2 camera, a B-2A Nikon filter set (excitation 450–490 nm bandpass filter, dichromatic mirror 500 nm cut-on, emission 520 nm longpass filter), and Nikon NIS-Elements software (Coherent Scientific, Australia). Sections were scanned using an automatic stage control setting that generated a grid pattern of images covering a set area. All fluorescence images were taken at  $10\times$  magnification with 100-ms exposure time. H&E-stained sections were captured under bright field. To estimate the level of oxidized thiols in muscle section by image analysis using ImageJ (version 1.44o; Wayne Rasband, National Institutes of Health, USA), the green channel of an 8-bit RGB image was used. For each scanned section, three images were selected for image analysis. Images with tissue edge artifacts or other obvious artifacts were discarded. The three selected fluorescence images were quantified and average fluorescence intensity (arbitrary unit) was calculated for the section. Section 1 was used to estimate reduced protein thiols, section 2 was used to estimate oxidized protein thiols, and section 3 was used to correct for a background signal. The oxidized percentages (intensity) of muscle sample were calculated as described in Fig. 1.

To measure intensive protein thiol oxidation, areas of intensive protein thiol oxidation were first identified by applying a threshold value (Fig. 6A, images i and ii). The threshold value was calculated using a technique modified from Tohma et al. [17]. In brief, the intensity distribution of low-intensity pixels from regions not showing intensive protein thiol oxidation was plotted (Fig. 6B). The threshold value was calculated as the mean pixel intensity  $\times$  3 standard deviations of the distribution. This accounted for 99.7% of low-intensity pixels.

#### Protein thiol oxidation using tissue homogenates

Reduced and oxidized protein thiols were measured using a dual labeling technique as described in detail elsewhere [12–14]. In brief, frozen quadriceps muscle was crushed under liquid nitrogen and protein was extracted with 20% TCA/acetone. Protein was solubilized in 0.5% sodium dodecyl sulfate, 0.5 M Tris at pH 7.3 (SDS buffer) and protein thiols were labeled with FLm. After removal of the unbound dye using ethanol, protein was resolubilized in SDS buffer, pH 7.0, and oxidized thiols were reduced with TCEP before the subsequent unlabeled reduced thiols were labeled with a second tag, the fluorescent dye Texas Red C2-maleimide (Invitrogen, USA). The sample was washed in ethanol and resuspended in SDS buffer. Samples were read using a fluorescence plate reader (Fluostar Optima; BMG Labtech) with wavelengths set at excitation 485 nm, emission 520 nm for FLm and excitation 595 nm, emission 610 nm for Texas red. A standard curve for each dye was created and results were expressed per milligram of protein, quantified using the Detergent Compatible protein assay (Bio-Rad).

#### Statistical analysis

All data are expressed as means  $\pm$  SEM. Statistical analysis was carried out in KaleidaGraph version 4.1.2. Comparisons of means

for two groups used Student's independent samples *t* test, and comparisons for more than three groups used one-way ANOVA. Tukey's significant difference was used as the post hoc test when significant results were seen in the ANOVA. Results were considered significant with  $p < 0.05$ .

## Results

#### Optimization of labeling method

Detection of protein thiols involved labeling serial cross sections of muscle with the fluorescent dye FLm or blocking protein thiols with NEM (Fig. 1). FLm was chosen as the labeling dye because it was specific for thiol groups, was relatively stable in the light, was cost effective, and gave a low nonspecific background signal [12]. The steps involved in the labeling method that were optimized include labeling of protein thiols with FLm, blocking of protein thiols with NEM, reduction of oxidized protein thiols with TCEP, and then labeling of protein thiols with FLm (Fig. 1). For the quantitative estimation of protein thiol oxidation, there was a correction for background signal caused by nonspecific binding by FLm (see equation in Fig. 1).

#### FLm labeling

Fixation of tissue is typically a primary step in histological protocols. However, thiols are readily oxidized by ambient oxygen [18–20]. To prevent artifactual oxidation, the compatibility of adding thiol-binding dye (FLm) in conjunction with the tissue fixation reagent (PFA) was examined. In the presence of 0.5 and 2.0% PFA there was substantial interference with FLm labeling (Fig. 2A). An alternate approach was to label with FLm before tissue fixation, but this has the potential to cause a loss of structural integrity. To test if FLm could be applied successfully before PFA fixation, sections were incubated with FLm in 0.5 M Tris–HCl, pH 7.0, before PFA treatment. For comparative purposes, tissue sections were also treated with PBS (Fig. 2B, image ii) to cause a loss of structure that was not evident in tissue sections treated with PFA (Fig. 2B, image i). For tissue sections treated with FLm in 0.5 M Tris–HCl, pH 7 (Fig. 2B, image iii), structural details were comparable to those of sections treated with PFA (Fig. 2B, image i), indicating that structural integrity is maintained when sections are treated with FLm before PFA fixation. Tissue fixation with PFA after FLm labeling had the potential to interfere with FLm signal. This was tested, and the FLm signal after fixation with PFA ( $35.7 \pm 1.8$  A.U.,  $n = 3$ ) was comparable to the FLm signal in the absence of PFA ( $36.4 \pm 3.3$  A.U.,  $n = 3$ ).

The completeness of FLm labeling was tested by extending the time of incubation and by incubating tissue sections with increasing concentrations of FLm. Labeling with FLm was complete in 30 min and the signal was stable for at least 120 min (Fig. 2C). A concentration of 0.225 mM FLm was sufficient for maximal labeling (Fig. 2D). After PFA fixation, overnight washing was used to remove PFA. For reduced protein thiols, samples were stored while the samples for oxidized protein thiols and background signal were prepared (Fig. 1). The effect of storage was tested, and the FLm signal after 24 h of storage at 4 °C in the dark ( $29.5 \pm 1.6$  A.U.,  $n = 3$ ) was comparable to the FLm signal without storage ( $29.0 \pm 0.5$  A.U.,  $n = 3$ ).

Based on these observations, the following protocol for FLm labeling was utilized. Immediately after the cutting of a transverse section at  $-20$  °C to minimize artifactual oxidation, the section was labeled with 0.225 mM FLm for 0.5 h at room temperature. The tissue section was then fixed for 0.5 h with 4% PFA.

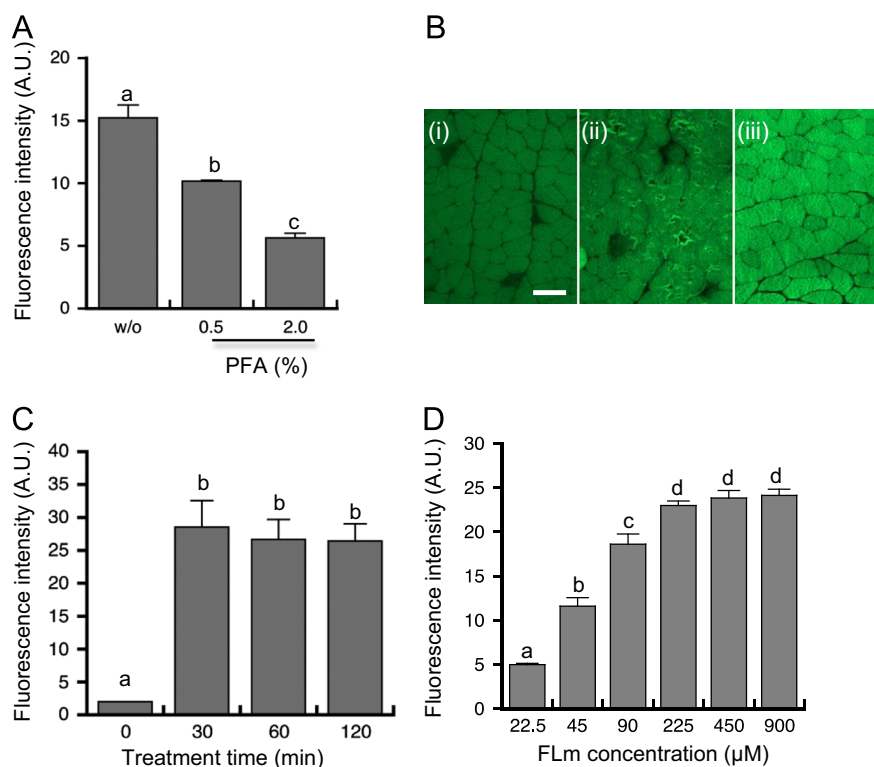


**Fig. 2.** Optimizing the FLm fluorescent label with C57 quadriceps muscles. (A) Fluorescence intensity of FLm after treatment without (w/o) or with 0.5 or 2% PFA. (B) Fluorescence images from three different labeling protocols: (i) the section was fixed with PFA, washed in PBS overnight to remove PFA, and then labeled with FLm in Tris–HCl, pH 7, for 30 min; (ii) the section was treated with PBS for 30 min, fixed with PFA, washed in PBS overnight to remove PFA, and then labeled with FLm in Tris–HCl, pH 7, for 30 min; (iii) the section was labeled with FLm in Tris–HCl, then treated with PFA, and then washed overnight in PBS. FLm and PFA concentrations were 0.225 mM and 4%, respectively. The images have been enhanced to show structural details. Scale bar, 100  $\mu$ m. (C) Effect of treatment time with FLm (0.225 mM) on fluorescence intensity. (D) Effect of FLm concentration on fluorescence intensity. For (A), (C), and (D), values without a common letter differ significantly;  $p < 0.05$ .  $n = 3$  mice.

#### Blocking of free protein thiols with NEM

NEM was used as a nonfluorescent thiol blocking agent for the measurement of background signal and oxidized protein thiols. To test the effectiveness of the NEM blocking reaction, tissue sections were incubated with FLm after incubating for 0.5 h with varying concentrations of NEM. Concentrations above 10 mM NEM were effective (Fig. 3A). To further examine the completeness of the NEM blocking reaction, the fluorescence intensity of multiple muscle fibers was measured. There was less scatter in fluorescence intensities in the presence of 200 mM NEM relative to lower concentrations of NEM (Fig. 3C). This was consistent with 200 mM NEM giving a more complete blocking reaction and, as a consequence, the time required for the blocking reaction was tested with 200 mM NEM. Blocking was complete in 30 min and stable for at least 120 min (Fig. 3B). Based on these observations, protein thiols were blocked for 30 min at a final concentration of 200 mM NEM in the FLm labeling protocol (Fig. 1).

NEM was not completely effective in blocking labeling by FLm, as some residual signal was evident after incubating with 200 mM NEM (Fig. 3A, w/o signal). This was attributed to nonspecific binding by FLm. Consequently, a correction for this background signal (Fig. 1) was incorporated into the labeling protocol.

#### Reduction with TCEP

To label oxidized protein thiols, tissue sections were first incubated with NEM to block preexisting protein thiols (Fig. 1). Sections were then incubated with the reducing agent (TCEP) to convert oxidized protein thiols to reduced protein thiols. TCEP has previously been shown to be an effective and stable reducing agent, with minimal interference with maleimide dyes when treated appropriately [12,21]. To test the effectiveness of TCEP,

tissue sections were incubated with FLm after incubating for 30 min with varying concentrations of TCEP (10–400 mM). Maximum reduction was achieved with 200 mM TCEP (Fig. 3D) and an incubation time of 60 min, with a stable signal for up to 180 min (Fig. 3E).

#### Technique verification

##### Signal consistency of consecutive muscle sections

To quantify the extent of protein thiol oxidation, the histological thiol-labeling technique utilized three muscle sections. Two consecutive 9- $\mu$ m sections were used for the measurement of reduced and oxidized protein thiols with the third section used to measure background signal (Fig. 1). For this approach to be quantitative, there needs to be a consistent level of oxidation between the two consecutive sections. This was tested and the level of oxidized protein thiols was comparable between two consecutive muscle sections (Fig. 4A, i and ii).

##### Detecting reversible oxidation of protein thiols

The histological thiol-labeling technique was designed to detect reversible oxidation of protein thiols caused by oxidative stress (Fig. 4B and C). To establish whether the technique was capable of detecting increased protein thiol oxidation, tissue sections were incubated with diamide, a reagent that causes the oxidation of thiols to disulfides [22]. In tissue sections not incubated with diamide, most protein thiols were in the reduced form (Fig. 4C) and were calculated (Fig. 1 for details) to be  $8.4 \pm 0.4\%$  oxidized. After a 60-min incubation with 5 mM diamide, there was a decrease in reduced protein thiols and a compensatory increase in oxidized protein thiols (Fig. 4C) and the thiols were calculated

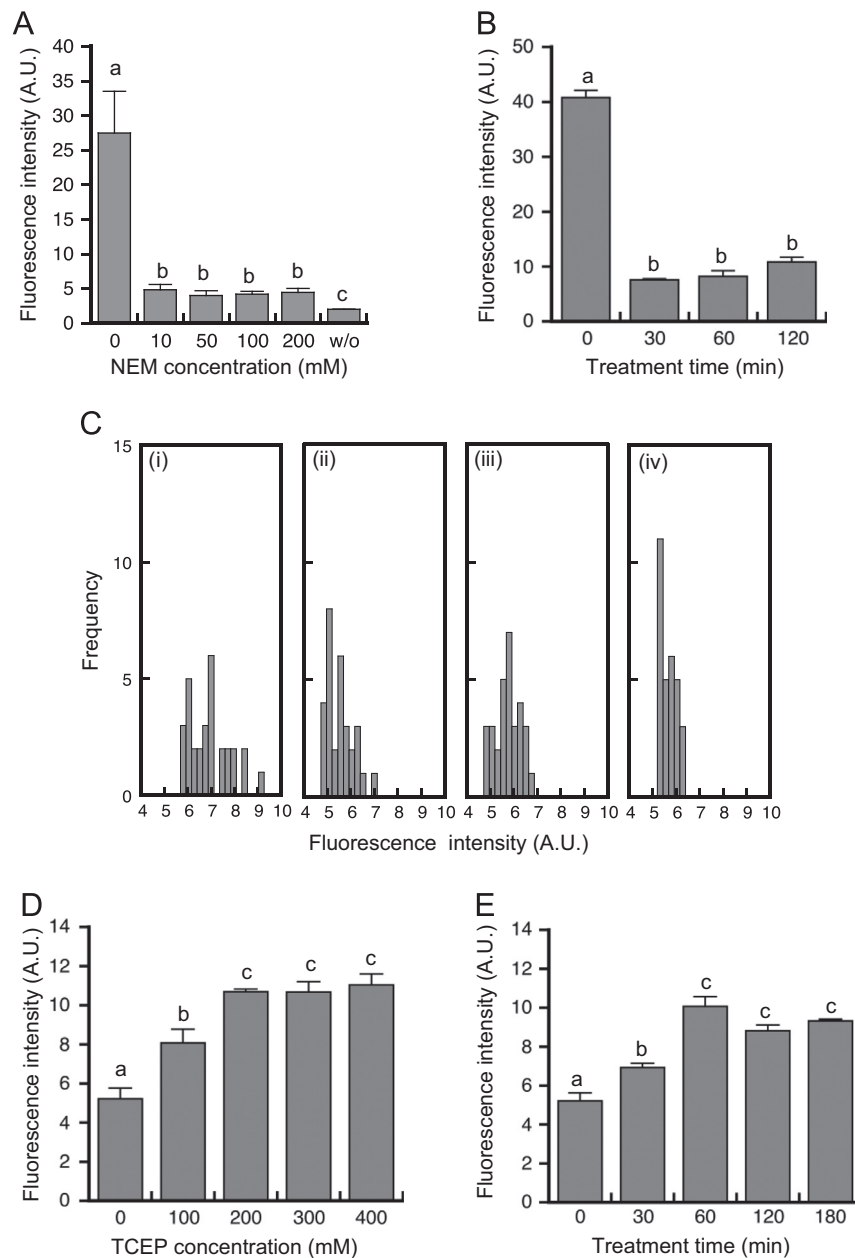


**Fig. 3.** Optimizing measurement of oxidized protein thiols in C57 quadriceps muscles. (A) Effectiveness of NEM blocking reaction. The sections were immersed in NEM solutions for 30 min. Background signal (w/o) was measured by omitting FLm treatment. (B) Effect of NEM treatment times on fluorescence intensity. Sections were labeled with FLm after treatment with 200 mM NEM. (C) Representative histograms of fluorescence intensity in muscle sections after blocking free thiol groups with four different NEM concentrations: (i) 10 mM, (ii) 50 mM, (iii) 100 mM, and (iv) 200 mM NEM.  $n = 3$  muscles, 10 muscle fibers per muscle (30 fibers in total) in each graph. (D) Effect of TCEP concentration on fluorescence intensity of oxidized thiols. After 30 min of TCEP treatment, sections were labeled with FLm. (E) Effect of increasing TCEP (200 mM) treatment time on fluorescence intensity of oxidized thiols. After TCEP (200 mM) treatment, all sections were stained with 0.225 mM FLm. For (A), (B), (D), and (E), values without a common letter differ significantly;  $p < 0.05$ .  $n = 3$  mice.

(Fig. 1 for details) to be  $86.9 \pm 1.2\%$  oxidized. This result indicates that changes in protein thiol oxidation could be detected and quantified.

#### Technique application

To demonstrate the practical use of this histology thiol-labeling technique, the level of protein thiol oxidation was examined in tissue sections from the dystrophic muscles of mdx mice. Mdx mice are a model for the human disease Duchenne muscular dystrophy, and we have previously shown that total protein thiol oxidation was elevated in quadriceps muscles using a quantitative dual-labeling technique we developed for whole muscle extracts

[2,12,13]. Two distinct patterns of protein thiol oxidation were evident in histological sections of mdx quadriceps muscles. First, the level of protein thiol oxidation was consistently elevated in all dystrophic myofibers compared with nondystrophic C57 myofibers (Fig. 5A). Protein thiol oxidation in mdx myofibers was  $19 \pm 3\%$ , and this was almost twofold higher than the level of  $10 \pm 1\%$  ( $n = 3$ ,  $p < 0.05$ ) in C57 myofibers.

The second pattern of protein thiol oxidation in dystrophic quadriceps muscles was heterogeneous localization of intensive protein thiol oxidation that was substantially higher than that of surrounding tissue (Fig. 5B, image iii). Intensive protein thiol oxidation was calculated (Fig. 1 for details) to be  $70 \pm 9\%$  ( $n = 5$ ) and occupied  $4.5 \pm 0.7\%$  ( $n = 3$ ) of the visualized tissue area (Fig. 6).

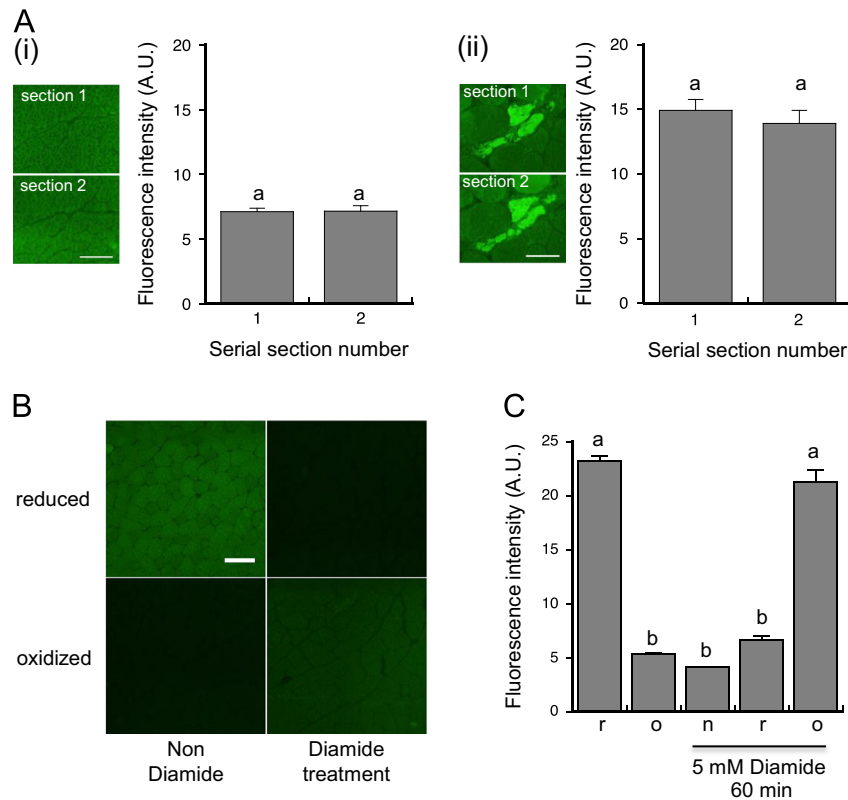


**Fig. 4.** Measuring oxidized protein thiols in quadriceps muscles. (A) Fluorescence intensity of oxidized thiols in consecutive serial sections (1 and 2). Representative images show consistency of (i) protein thiol oxidation and (ii) intense protein thiol oxidation in two consecutive serial sections.  $n = 3$  mdx mice. (B) Representative images of tissue sections of C57 muscle without and with diamide treatment. (C) Treatment with diamide before labeling with the histology thiol protocol. Symbols: r, reduced thiols; o, oxidized thiols; and n, background signal.  $n = 3$  C57 mice. Scale bars, 100  $\mu$ m. The images have been consistently enhanced to show structural details. For (A) and (C), values without a common letter differ significantly;  $p < 0.05$ .

These regions contained myofibers with fragmented sarcoplasm and increased number of mononucleated cells, indicative of early stages of myofiber damage [23]. It was evident from longitudinal muscle sections that intensive protein thiol oxidation was specific to individual myofibers (Fig. 5C). In dystrophic muscles we also observed regions with an advanced stage of necrosis (Fig. 5B, image viii), which contained many mononucleated cells (presumably inflammatory cells), myofibers with extensive sarcoplasmic fragmentation, and small newly regenerated centrally nucleated myotubes. These areas did not display intensive protein thiol oxidation (Fig. 5B, image vii). Taken together our data indicate that intensive protein thiol oxidation reflects an early stage of myofiber damage.

To establish whether the patterns of protein thiol oxidation observed in quadriceps muscles were also evident in other muscles, the triceps muscles of dystrophic mice were examined. As observed with quadriceps muscles, there was consistent elevation in protein thiol oxidation in mdx triceps. Heterogeneous regions of intensive protein thiol oxidation were also present (Fig. 7, images iii and vii), and protein thiol oxidation was similarly elevated in myofibers in which there was evidence of early, but not late, myofiber damage (Fig. 7, images iv and viii).

Quantitative data generated using the histology thiol-labeling technique was compared with a different technique (2tag) previously developed to measure the extent of protein thiol oxidation in whole-muscle extracts, rather than tissue sections [12]. The level of protein thiol oxidation was comparable (not significantly different) between the histology thiol-labeling technique ( $9.7 \pm 0.7\%$ ,  $n = 6$ ) and the dual-labeling method ( $7.3 \pm 1.0\%$ ,  $n = 6$ ) measured in triceps of C57 mice. The level of protein thiol oxidation was also comparable between the histology thiol-labeling technique

( $14.8 \pm 2\%$ ,  $n = 10$ ) and the dual-labeling method measured in triceps of mdx mice ( $17.1 \pm 1.1\%$ ,  $n = 7$ ). These data indicate that the histology thiol-labeling technique provides reliable quantitative information as to the level of protein thiol oxidation in muscle.

## Discussion

We have developed a fluorescence histology technique to assess the extent of reversible protein thiol oxidation in tissue sections. The key advantage is that it provides information on regional variations in protein thiol oxidation. This technique complements a dual-labeling method we developed to quantify the extent of total protein thiol oxidation in tissue extracts [12].

One of the difficulties in measuring protein thiol oxidation is that thiols are sensitive to oxidation during sample preparation. Consequently, to prevent artifactual oxidation, protein thiol groups were labeled or blocked before tissue fixation. There was no loss in structural integrity in adopting this procedure, possibly a result of blocking the activity of endogenous proteases by binding cysteine residues [24]. Other techniques examining aspects of protein thiol oxidation have not incorporated this precaution [25,26].

Thiol oxidation can result in the formation of protein nitrosothiols, intermolecular and intramolecular disulfide bonds in proteins, and disulfides with low-molecular-weight compounds such glutathione and cysteine [27]. These modifications are biologically reversible and, because TCEP is used as the reducing agent, all of these changes can be detected with the protein histology thiol-labeling technique. Consequently, the histology thiol technique should be useful because it is a relatively simple and cost-effective assay that can be used as a scanning technique

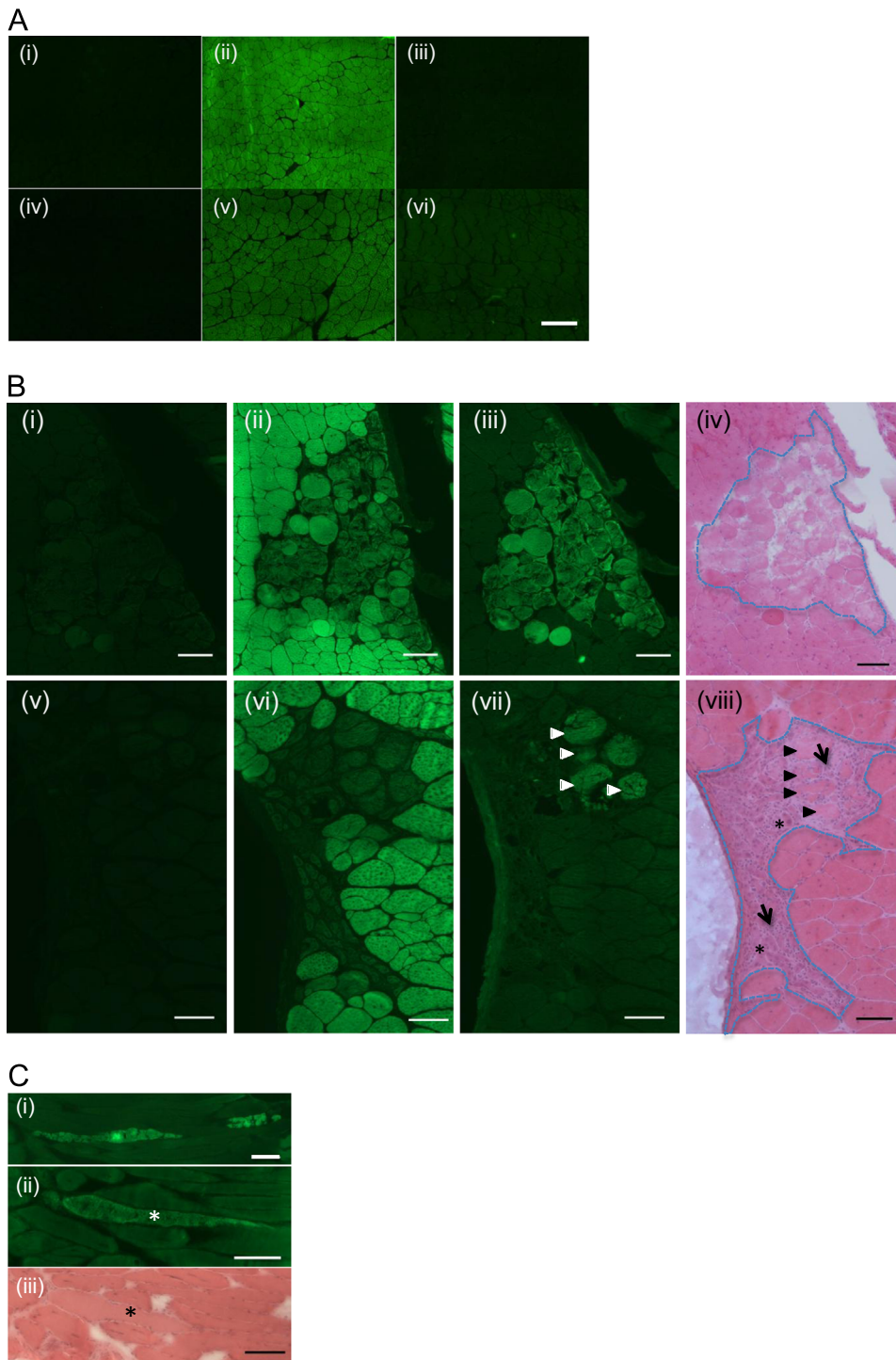


**Fig. 5.** Representative images of C57 and mdx quadriceps muscles. (A) Fluorescence images of FLM-labeled C57 (i–iii) and mdx (iv–vi) quadriceps muscles. Images are shown for the background signal (i and iv), reduced protein thiols (ii and v), and oxidized protein thiols (iii and vi). Scale bar, 200  $\mu$ m. (B) Intensive protein thiol oxidation at the early necrosis stage (i–iv) and at the later necrosis stage (v–viii) in mdx quadriceps muscles. Images are shown for background signal (i and v), reduced protein thiols (ii and vi), oxidized protein thiols (iii and vii), and H&E stain (iv and viii). Areas that show myofibers with fragmented sarcoplasm and few inflammatory cells (iv) and areas with extensive sarcoplasmic fragmentation and inflammation (viii) are outlined. Arrowheads indicate myofibers with fragmented sarcoplasm, arrows indicate inflammatory cells, and asterisks indicate newly formed centrally nucleated myotubes. Scale bars, 100  $\mu$ m. (C) Representative longitudinal images of myofibers with oxidized protein thiols from two different mdx quadriceps muscles (i and ii). Asterisks indicate the same fiber in (ii) and the H&E image (iii). Scale bars, 100  $\mu$ m. The images have been enhanced to show structural details.

to detect multiple types of protein thiol oxidation. In some circumstances, such as glutathionylation, other visualization techniques could be used to identify the type of thiol oxidation [25], although this technique does not appear to have been tested with tissue.

The histology thiol-labeling technique involved labeling both reduced and oxidized protein thiols rather than using a single labeling protocol for either reduced or oxidized proteins. Although this approach required additional effort, it enabled oxidized protein thiol content to be expressed as a percentage of total

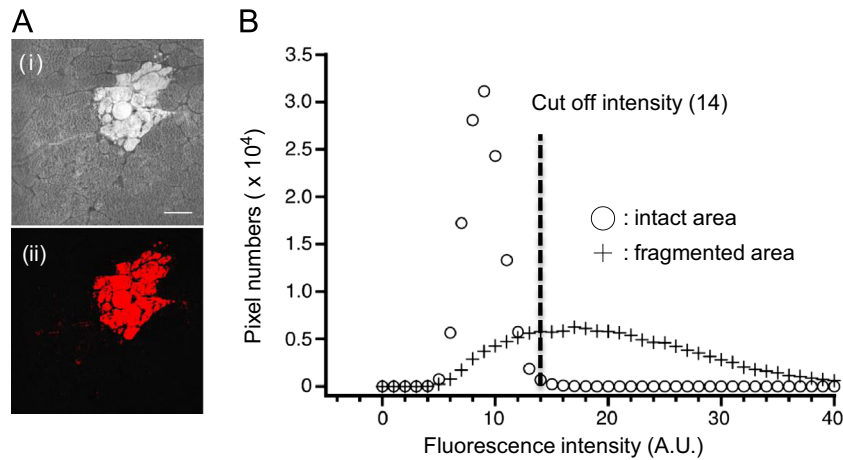


**Fig. 6.** Quantification of intensive protein thiol oxidation in mdx quadriceps muscles. (A) (i) Representative image showing oxidized protein thiols and (ii) same image after setting the threshold parameters. The red image was used for quantification. Scale bar, 100  $\mu\text{m}$ . (B) Representative histogram comparing fluorescence intensity of “intact” dystrophic myofibers (intact area), containing low levels of oxidized protein thiols, with a necrotic area (fragmented area) containing intensively oxidized protein thiols. (For interpretation of the references to color in this figure legend, the reader is referred to the web version of this article.)

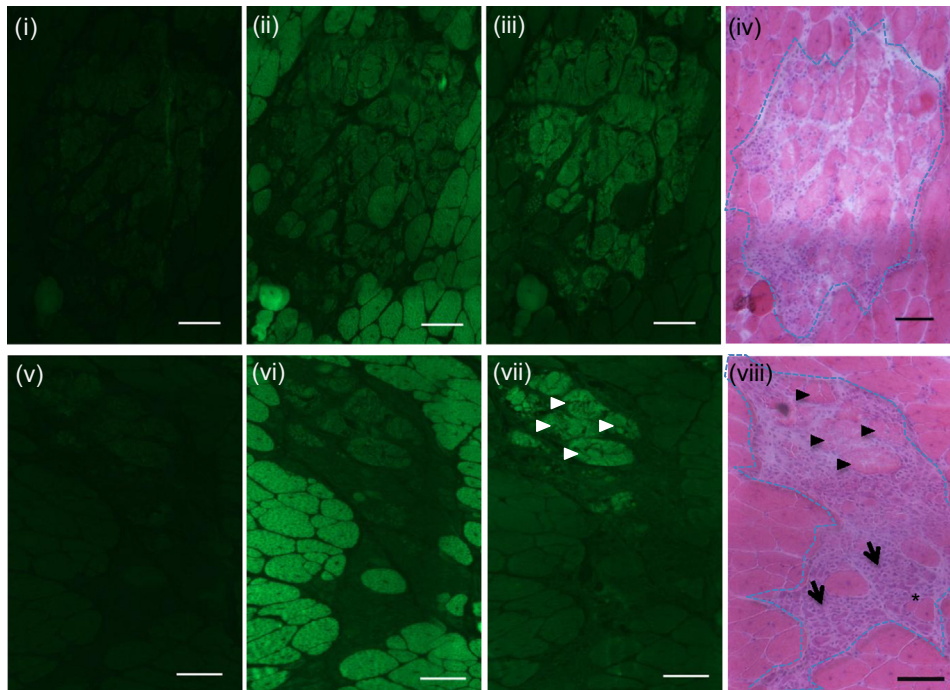


**Fig. 7.** Protein thiol oxidation in mdx triceps muscles. Intensive protein thiol oxidation at the early stage of necrosis (i–iv) and at the later necrosis stage (v–viii) in mdx triceps muscles. Images are shown for background signal (i and v), reduced protein thiols (ii and vi), oxidized protein thiols (iii and vii), and H&E stain (iv and viii). Areas that show myofibers with fragmented sarcoplasm and few inflammatory cells (iv) and areas with extensive sarcoplasmic fragmentation and inflammation (viii) are outlined. Arrowheads indicate myofibers with fragmented sarcoplasm, arrows show inflammatory cells, and asterisks indicate newly formed centrally nucleated myotubes. Some degenerating myofibers (arrowheads) show intensive protein thiol oxidation. Scale bars, 100  $\mu\text{m}$ . The images have been enhanced to show structural details.

protein thiols. This quantitative approach has the key advantage that it allows data from independent experiments to be compared, as discussed in El-Shafey et al. [2]. We have previously compared oxidative stress and damage measures in mdx and control muscles, including glutathione oxidation and oxidative damage to lipid and proteins, and we have established that in this model, protein thiols seem to be especially sensitive to oxidative stress [2]. Therefore the histology thiol-labeling technique can be used as a screening tool to identify tissues susceptible to such oxidative stress. Where changes in the level of global protein thiol oxidation are detected, further work using more specific proteomic techniques can be used to identify the particular proteins that have been modified by such oxidative stress [28].

The usefulness of the new histology thiol technique that shows the location of protein thiol oxidation is illustrated in its application to dystrophic mdx muscles *in vivo*, in which it was evident that there was a consistent increase in protein thiol oxidation within dystrophic myofibers (compared with nondystrophic muscles), rather than elevated protein thiol oxidation being conspicuous within some but not all dystrophic myofibers or elevated in interstitial cells. Because protein thiol oxidation has the potential to affect the function of multiple proteins, this observation implies that metabolic processes may be affected in all of the dystrophic mdx myofibers.

A striking observation of the histology thiol-labeling technique was the identification of regions of intensive protein thiol oxidation



within different myofibers. Dystrophic limb muscles of adult mdx mice are characterized by low levels (~6% of the total area) of ongoing necrosis and inflammation with subsequent regeneration [14]. We established that the regions of intensive protein thiol oxidation were associated with early myonecrosis and inflammation, but not later stages of this process, when more inflammatory cells were present. The regions of intense protein thiol oxidation staining appear in H&E sections as regions that contain pale myofibers with fragmented sarcoplasm. We have previously shown that such myofibers also exhibit “leaky” sarcolemma that lost integrity, an early sign of myofiber damage [23]. In this context, the intensive protein thiol oxidation could be a transient consequence of increased oxidative stress caused by increased intracellular calcium as the cell membrane loses integrity [18]. This is of interest because ROS have been shown to activate several proteolytic pathways contributing to the degradation of damaged muscle cells [11]. Particularly relevant are observations that increased protein oxidation results in the degradation of myofibrillar proteins by calpain I, calpain II, and caspase-3 [29]. Consequently, it would be of interest to establish whether intensive protein thiol oxidation is an early event in focal breakdown of dystrophic myofibers.

Oxidative stress is an area of active investigation in many fields of research, but a lack of experimental tools has made it challenging to investigate protein thiol oxidation in situ in organs and tissue from animals and humans. The development of our histology thiol-labeling technique and its application to dystrophic muscle tissue sections show the benefits of being able to visualize reversible protein thiol oxidation in histological samples. Many organs have a complex composition of cell types, thus imaging analysis of the location of protein thiol oxidation on tissue histology sections will help to delineate how oxidative stress affects protein function in complex tissues.

## References

- [1] Halliwell, B.; Gutteridge, J. M. C. *Free Radicals in Biology and Medicine*. Oxford; New York: Oxford University Press; 2007.
- [2] El-Shafey, A. F.; Armstrong, A. E.; Terrill, J. R.; Grounds, M. D.; Arthur, P. G. Screening for increased protein thiol oxidation in oxidatively stressed muscle tissue. *Free Radic Res* **45**:991–999; 2011.
- [3] Halliwell, B.; Whiteman, M. Measuring reactive species and oxidative damage in vivo and in cell culture: how should you do it and what do the results mean? *Br J Pharmacol* **142**:231–255; 2004.
- [4] Kadiiska, M. B.; Gladen, B. C.; Baird, D. D.; Germolec, D.; Graham, L. B.; Parker, C. E.; Nyska, A.; Wachsman, J. T.; Ames, B. N.; Basu, S.; Brot, N.; Fitzgerald, G. A.; Floyd, R. A.; George, M.; Heinecke, J. W.; Hatch, G. E.; Hensley, K.; Lawson, J. A.; Marnett, L. J.; Morrow, J. D.; Murray, D. M.; Plataras, J.; Roberts 2nd L. J.; Rokach, J.; Shigenaga, M. K.; Sohal, R. S.; Sun, J.; Tice, R. R.; Van Thiel, D. H.; Wellner, D.; Walter, P. B.; Tomer, K. B.; Mason, R. P.; Barrett, J. C. Biomarkers of oxidative stress study II: are oxidation products of lipids, proteins, and DNA markers of CCl<sub>4</sub> poisoning? *Free Radic Biol Med* **38**:698–710; 2005.
- [5] Milne, G. L.; Sanchez, S. C.; Musiek, E. S.; Morrow, J. D. Quantification of F<sub>2</sub>-isoprostanes as a biomarker of oxidative stress. *Nat Protoc* **2**:221–226; 2007.
- [6] Lui, J. K. C.; Lipscombe, R.; Arthur, P. G. Detecting Changes in the Thiol Redox State of Proteins Following a Decrease in Oxygen Concentration Using a Dual Labeling Technique. *J. Proteome Res* **9**:383–392; 2010.
- [7] Biswas, S.; Chida, A. S.; Rahman, I. Redox modifications of protein-thiols: emerging roles in cell signaling. *Biochemical pharmacology* **71**:551–564; 2006.
- [8] Wang, Y.; Yang, J.; Yi, J. Redox sensing by proteins: oxidative modifications on cysteines and the consequent events. *Antioxid Redox Signal* **16**:649–657; 2012.
- [9] Droge, W. Free radicals in the physiological control of cell function. *Physiological reviews* **82**:47–95; 2002.
- [10] Leonard, S. E.; Reddie, K. G.; Carroll, K. S. Mining the thiol proteome for sulfenic acid modifications reveals new targets for oxidation in cells. *ACS chemical biology* **4**:783–799; 2009.
- [11] Powers, S. K.; Duarte, J.; Kavazis, A. N.; Talbert, E. E. Reactive oxygen species are signalling molecules for skeletal muscle adaptation. *Exp Physiol* **95**:1–9; 2010.
- [12] Armstrong, A. E.; Zerbes, R.; Fournier, P. A.; Arthur, P. G. A fluorescent dual labeling technique for the quantitative measurement of reduced and oxidized protein thiols in tissue samples. *Free radical biology & medicine* **50**:510–517; 2011.
- [13] Terrill, J. R.; Radley-Crabb, H. G.; Grounds, M. D.; Arthur, P. G. N-Acetylcysteine treatment of dystrophic mdx mice results in protein thiol modifications and inhibition of exercise induced myofibre necrosis. *Neuromuscular disorders: NMD* **22**:427–434; 2012.
- [14] Radley-Crabb, H.; Terrill, J.; Shavliakadze, T.; Tonkin, J.; Arthur, P.; Grounds, M. A single 30 min treadmill exercise session is suitable for ‘proof-of concept studies’ in adult mdx mice: a comparison of the early consequences of two different treadmill protocols. *Neuromuscular disorders: NMD* **22**:170–182; 2012.
- [15] Soderdahl, T.; Enoksson, M.; Lundberg, M.; Holmgren, A.; Ottersen, O. P.; Orrenius, S.; Bolcsfoldi, G.; Cotgreave, I. A. Visualization of the compartmentalization of glutathione and protein-glutathione mixed disulfides in cultured cells. *FASEB J* **17**:124–126; 2003.
- [16] Terrill, J. R.; Radley-Crabb, H. G.; Iwasaki, T.; Lemckert, F. A.; Arthur, P. G.; Grounds, M. D. Oxidative stress and pathology in muscular dystrophies: focus on protein thiol oxidation and dysferlinopathies. *The FEBS journal* **280**:4149–4164; 2013.
- [17] Tohma, H.; Hepworth, A. R.; Shavliakadze, T.; Grounds, M. D.; Arthur, P. G. Quantification of ceroid and lipofuscin in skeletal muscle. *The journal of histochemistry and cytochemistry: official journal of the Histochemistry Society* **59**:769–779; 2011.
- [18] Arthur, P. G.; Grounds, M. D.; Shavliakadze, T. Oxidative stress as a therapeutic target during muscle wasting: considering the complex interactions. *Curr Opin Clin Nutr Metab Care* **11**:408–416; 2008.
- [19] Rossi, R.; Milzani, A.; Dalle-Donne, I.; Giustarini, D.; Lusini, L.; Colombo, R.; Di Simplicio, P. Blood glutathione disulfide: in vivo factor or in vitro artifact? *Clin Chem* **48**:742–753; 2002.
- [20] Rogers, L. K.; Leinweber, B. L.; Smith, C. V. Detection of reversible protein thiol modifications in tissues. *Anal Biochem* **358**:171–184; 2006.
- [21] Getz, E. B.; Xiao, M.; Chakrabarty, T.; Cooke, R.; Selvin, P. R. A comparison between the sulfhydryl reductants tris(2-carboxyethyl)phosphine and dithiothreitol for use in protein biochemistry. *Anal Biochem* **273**:73–80; 1999.
- [22] Kosower, N. S.; Kosower, E. M.; Wertheim, B.; Correa, W. S. Diamide, a new reagent for the intracellular oxidation of glutathione to the disulfide. *Biochem Biophys Res Commun* **37**:593–596; 1969.
- [23] Shavliakadze, T.; White, J.; Hoh, J. F.; Rosenthal, N.; Grounds, M. D. Targeted expression of insulin-like growth factor-I reduces early myofiber necrosis in dystrophic mdx mice. *Molecular therapy: the journal of the American Society of Gene Therapy* **10**:829–843; 2004.
- [24] Thomas, J. A.; Mallis, R. J. Aging and oxidation of reactive protein sulfhydryls. *Exp Gerontol* **36**:1519–1526; 2001.
- [25] Cotgreave, I. A.; Goldschmidt, L.; Tonkonogi, M.; Svensson, M. Differentiation-specific alterations to glutathione synthesis in and hormonally stimulated release from human skeletal muscle cells. *FASEB journal: official publication of the Federation of American Societies for Experimental Biology* **16**:435–437; 2002.
- [26] Mastroberardino, P. G.; Orr, A. L.; Hu, X.; Na, H. M.; Greenamyre, J. T. A FRET-based method to study protein thiol oxidation in histological preparations. *Free radical biology & medicine* **45**:971–981; 2008.
- [27] Ghezzi, P. Oxidoreduction of protein thiols in redox regulation. *Biochemical systematics transactions* **33**:1378–1381; 2005.
- [28] Leichert, L. I.; Gehrke, F.; Gudiseva, H. V.; Blackwell, T.; Ilbert, M.; Walker, A. K.; Strahler, J. R.; Andrews, P. C.; Jakob, U. Quantifying changes in the thiol redox proteome upon oxidative stress in vivo. *Proc Natl Acad Sci U S A* **105**:8197–8202; 2008.
- [29] Smuder, A. J.; Kavazis, A. N.; Hudson, M. B.; Nelson, W. B.; Powers, S. K. Oxidation enhances myofibrillar protein degradation via calpain and caspase-3. *Free radical biology & medicine* **49**:1152–1160; 2010.